AMERICAN SOCIETY FOR MICROBIOLOGY | Infection and Immunity

Bacterial Dose-Dependent Role of G Protein-Coupled Receptor Kinase 5 in *Escherichia coli*-Induced Pneumonia

Nandakumar Packiriswamy,[b] Michael Steury,[a] Ian C. McCabe,[a] Scott D. Fitzgerald,[c] Narayanan Parameswaran[a,b]

Department of Physiology, Michigan State University, East Lansing, Michigan, USA[a]; Comparative Medicine and Integrative Biology Program, Michigan State University, East Lansing, Michigan, USA[b]; Department of Pathobiology and Diagnostic Investigation, Michigan State University, East Lansing, Michigan, USA[c]

G protein-coupled receptor kinase 5 (GRK5) is a serine/threonine kinase previously shown to mediate polymicrobial sepsis-induced inflammation. The goal of the present study was to examine the role of GRK5 in monomicrobial pulmonary infection by using an intratracheal *Escherichia coli* infection model of pneumonia. We used sublethal and lethal doses of *E. coli* to examine the mechanistic differences between low-grade and high-grade inflammation induced by *E. coli* infection. With a sublethal dose of *E. coli*, GRK5 knockout (KO) mice exhibited higher plasma CXCL1/KC levels and enhanced lung neutrophil recruitment early after infection, and lower bacterial loads, than wild-type (WT) mice. The inflammatory response was also diminished, and resolution of inflammation advanced, in the lungs of GRK5 KO mice. In contrast to the reduced bacterial loads in GRK5 KO mice following a sublethal dose, at a lethal dose of *E. coli*, the bacterial burdens remained high in GRK5 KO mice relative to those in WT mice. This occurred in spite of enhanced plasma CXCL1 levels as well as neutrophil recruitment in the KO mice. But the recruited neutrophils (following high-dose infection) exhibited decreased CD11b expression and reduced reactive oxygen species production, suggesting decreased neutrophil activation or increased neutrophil exhaustion in the GRK5 KO mice. In agreement with the increased bacterial burden, KO mice showed poorer survival than WT mice following *E. coli* infection at a lethal dose. Overall, our data suggest that GRK5 negatively regulates CXCL1/KC levels during bacterial pneumonia but that the role of GRK5 in the clinical outcome in this model is dependent on the bacterial dose.

Pneumonia is one of the leading causes of mortality in the United States and is a major cause of severe sepsis (1, 2). Acute lung injury (ALI) is often caused by infection with bacteria, viruses, or other organisms, including fungi and chlamydiae; of these, Gram-negative bacterial species are the dominant cause of pneumonia-induced ALI (3). As in any bacterial infection, neutrophil chemotaxis plays a vital role in clearing the infection. The migration and recruitment of neutrophils to the lung require the production of ELR^+ (glutamic acid-leucine-arginine) CXC chemokines, such as CXCL1/KC, CXCL2/MIP2, and CXCL5/LIX (4–6). In addition to the recruitment of neutrophils, the clearance of dying/dead neutrophils is also important in the resolution of bacterial infection-induced inflammation. Dysregulation of any of these processes can lead to detrimental outcomes (7). A key strategy in reducing mortality is to modulate the innate immune system so as to enhance the host's ability to combat microbial infection while carefully balancing the inflammatory response to limit tissue injury.

G protein-coupled receptor kinases (GRKs) are serine/threonine protein kinases discovered in the context of G protein-coupled receptor (GPCR) phosphorylation but later shown to have a wide range of receptor and nonreceptor targets (8). Seven GRKs (GRK1 to -7) have been identified in mammals and have been demonstrated to be critical in various physiological processes. Since its discovery in 1993 (9), GRK5 has been shown to mediate or inhibit signaling processes in a number of cellular systems. More recently, GRK5 has been shown to be a critical player in inflammatory responses in various animal models of disease as well as in cell culture studies (10–13). Furthermore, GRK5 levels have been shown to be modulated in different disease conditions, including neurodegenerative disorders (14), cancers (15), sepsis (16), and cardiac failure (17, 18). In recent studies, we showed that GRK5 is an important regulator of endotoxemia and polymicrobial sepsis pathogenesis (19, 20). Although GRK5 is highly expressed in normal (9, 21) and diseased (22) airways, its role in lung infection is unknown. Therefore, we tested the hypothesis that GRK5 is an important regulator of bacterial pneumonia. We demonstrate here that GRK5 significantly modulates plasma CXCL1/KC levels and neutrophil recruitment during bacterial pneumonia but that the outcome of pathogenesis is critically dependent on the dose of the bacteria.

MATERIALS AND METHODS

Materials. *Escherichia coli* (O6:B1) was obtained from the ATCC (Manassas, VA, USA). Protease inhibitor cocktail tablets were from Roche Applied Science (Indianapolis, IN, USA); antibodies against pIκBα and tubulin were from Cell Signaling Technology, Inc. (Danvers, MA, USA) and Sigma (St. Louis, MO, USA), respectively. Most cytokines and chemokines were from Peprotech (USA).

Experimental animals. GRK5 knockout (KO) mice and wild-type (WT) control mice described previously (20) were used in the study. Healthy male mice (8 to 12 weeks old) were used in the experiments. All mice were housed with a 12-h alternating light-dark cycle at 25°C, with

Received 18 January 2016 **Returned for modification** 20 February 2016
Accepted 6 March 2016

Accepted manuscript posted online 14 March 2016

Citation Packiriswamy N, Steury M, McCabe IC, Fitzgerald SD, Parameswaran N. 2016. Bacterial dose-dependent role of G protein-coupled receptor kinase 5 in *Escherichia coli*-induced pneumonia. Infect Immun 84:1633–1641. doi:10.1128/IAI.00051-16.

Editor: S. M. Payne

Address correspondence to Narayanan Parameswaran, narap@msu.edu.

Supplemental material for this article may be found at http://dx.doi.org/10.1128/IAI.00051-16.

50% humidity, and with free access to food and water. All experiments performed were approved by the Institutional Animal Care and Use Committee at Michigan State University and conformed to NIH guidelines.

Pulmonary infection model. A clinical isolate of *E. coli* (O6:B1; ATCC 25922) was used for lung infection in mice. *E. coli* was grown in Trypticase soy broth for 8 h at 37°C, and the bacterial CFU count of each culture was determined by comparing the specific OD_{600} (optical density at 600 nm) value to a standard curve. Bacteria were washed twice with sterile phosphate-buffered saline (PBS) and were adjusted to the appropriate final concentration. For bacterial injection, mice were anesthetized using xylazine (5 mg/kg) and ketamine (80 mg/kg), placed in an intubation stand, and gently secured by the incisors. The tongue was gently pulled out with a clean forceps to expose the epiglottis and trachea. With the tongue held in position, 50 μl of a bacterial inoculum was instilled (23). Mice of the different genotypes were injected in a blinded fashion. Sham intratracheal inoculation were also carried out with PBS, which served as a control. Mice were observed and euthanized at various time points up to 48 h for cell and tissue analysis.

Determination of bacterial loads. Mice infected with *E. coli* were euthanized 4, 12, or 24 h postinfection. Bronchoalveolar lavage (BAL) fluid, lungs, blood, and other organs were harvested aseptically. The postcaval lung lobe was collected, weighed, and homogenized in 1 ml of sterile PBS. All the samples were plated in Trypticase soy agar (BD Biosciences) and were incubated at 37°C for 24 h. CFU were counted to determine bacterial loads, which were expressed as log CFU per milliliter of blood, per 50 μl of BAL fluid, or per gram of lung.

***In vitro* bacterial killing assay.** Neutrophils were collected from the different groups of mice by processing peritoneal lavage fluid 4 h after thioglycolate injection. A small aliquot was separated in order to assess the purity of neutrophils by flow cytometry (purity was determined to be 95%). Neutrophils were enumerated and were incubated with opsonized *E. coli* for 30 min to enable bacterial uptake by neutrophils. Following incubation, cells were treated with gentamicin (200 μg) for 30 or 60 min to kill extracellular *E. coli*. The cells were then washed twice with PBS, and the pellet was lysed with 0.1% Triton X-100 and was plated onto tryptic soy agar. Plates were incubated at 37°C, and CFU were counted 24 h postplating.

Immune cell infiltration. Lungs, bronchoalveolar lavage fluid, and blood were collected at specified time points postinfection to measure the infiltration/composition of immune cells. The left lung lobe was collected and was incubated in a medium containing collagenase D (1 mg/ml) at 37°C for an hour with gentle shaking; then the tissue was disrupted to release cells. To determine changes in the number of cells, cells were counted using a hemocytometer. For flow cytometry, cells were also labeled with cell surface markers for various immune cells (Gr-1, CD11b, F4/80, CD11c, B220, CD3, and Ly6C), and data were acquired using an LSR II flow cytometer (BD Biosciences) and were analyzed using FlowJo software (Tree Star, Inc., Ashland, OR, USA) as described previously (19).

Chemokine receptor expression. Bone marrow neutrophils from mice were isolated using Percoll gradient centrifugation. Briefly, an erythrocyte (RBC)-lysed bone marrow cell suspension was gently layered on top of 62% Percoll solution and was centrifuged at 2,200 rpm for 30 min. At the end of the gradient centrifugation, the cloudy layer below the interface was collected and was gently washed twice. Neutrophil purity was assessed using flow cytometry. For the expression studies, neutrophils were treated with the chemokine ligand CXCL1 (100 ng) or CXCL2 (50 ng) for 10 or 5 min, respectively. Samples were then fixed immediately, processed, and analyzed by flow cytometry.

Cytokine/chemokine measurements. Plasma, tissue lysates from lung samples, and bronchoalveolar lavage fluid were analyzed by enzyme-linked immunosorbent assays (ELISA) for cytokine and chemokine levels using ELISA kits from eBioscience, Inc. as described previously (19). CXCL1 and CXCL2 levels were determined using ELISA kits from R&D Systems (Minneapolis, MN).

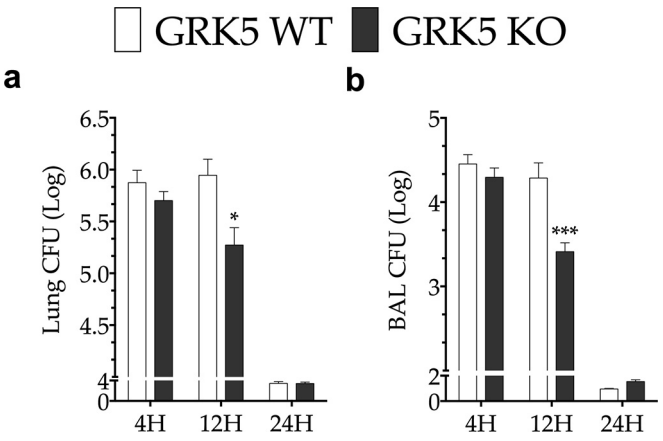

FIG 1 Bacterial burdens in mice with wild-type (WT) GRK5 and in GRK5 knockout (KO) mice following infection with a sublethal dose of *E. coli*. GRK5 WT and KO mice were injected intratracheally with 1×10^6 CFU of *E. coli*. After the time points indicated, lungs (a) and bronchoalveolar lavage fluid (b) were collected and were plated for bacterial growth as described in Materials and Methods. (Number of animals: 9 at 4 h, 12 at 12 h, and 7 at 24 h.) Asterisks indicate significant differences (*, $P < 0.05$; ***, $P < 0.001$) from the corresponding infected WT group.

Immunoblot analysis. Lung tissue samples for Western blot analysis were prepared by homogenizing the tissue in lysis buffer (1 M HEPES, 2 M KCl, 0.5 M EDTA, and 0.1 M EDTA along with protease and phosphatase inhibitors). The protein concentrations (Bradford) were determined, and equivalent amounts of protein were loaded onto the gels for Western blotting. Immunoblotting for pIκBα and tubulin was carried out as described previously (19). The bands were quantified using ImageJ (for chemiluminescence) or Li-Cor's Odyssey program (for fluorescence).

Measurement of reactive oxygen species (ROS) production. Cells from BAL fluid were collected 15 h postinfection from mice infected with *E. coli*. RBC lysis was carried out, and cells were counted and resuspended in PBS with 0.5% fetal bovine serum (FBS). Equal numbers of cells from wild-type and knockout mice were then loaded with carboxy-H_2DCFDA [5(6)-carboxy-2′,7′-dichlorodihydrofluorescein diacetate] dye (10 μM) for 60 min. The cells were then washed and were resuspended in PBS medium. The fluorescence from the cells was determined in a Tecan SpectraFluor Plus fluorescence plate reader (excitation of 400 nm and emission of 505 nm). Background fluorescence from the cells was subtracted from the fluorescence values obtained after loading of the cells with carboxy-H_2DCFDA dye. Data are expressed as fluorescence intensity.

Histopathology analysis. Lung tissue was collected in 10% (wt/vol) buffered formalin (Sigma) and was processed for hematoxylin and eosin staining as described previously (24). Histopathology analysis was performed by a board-certified veterinary pathologist (S.D.F) for the following parameters: interstitial lung inflammation, presence of bacteria, fibrin deposition, necrosis, pulmonary vein edema, and pleuritis. For each mouse, histopathological lesions were scored against a total possible score of 30 for each mouse, with points assigned as follows: presence of areas of necrosis, 10; presence of fibrin in the alveoli, 10; presence of bacteria in the alveoli, 5; evidence of alveolitis and pulmonary vein edema, 5.

Statistical analysis. All data are presented as means ± standard errors of the means (SEM). Two-group comparisons were performed using the Mann-Whitney test, and comparisons of more than two groups were carried out by ANOVA (analysis of variance) with the Bonferroni posttest. All statistical analyses were performed using GraphPad Prism software (GraphPad, San Diego, CA, USA), and P values of <0.05 were considered statistically significant.

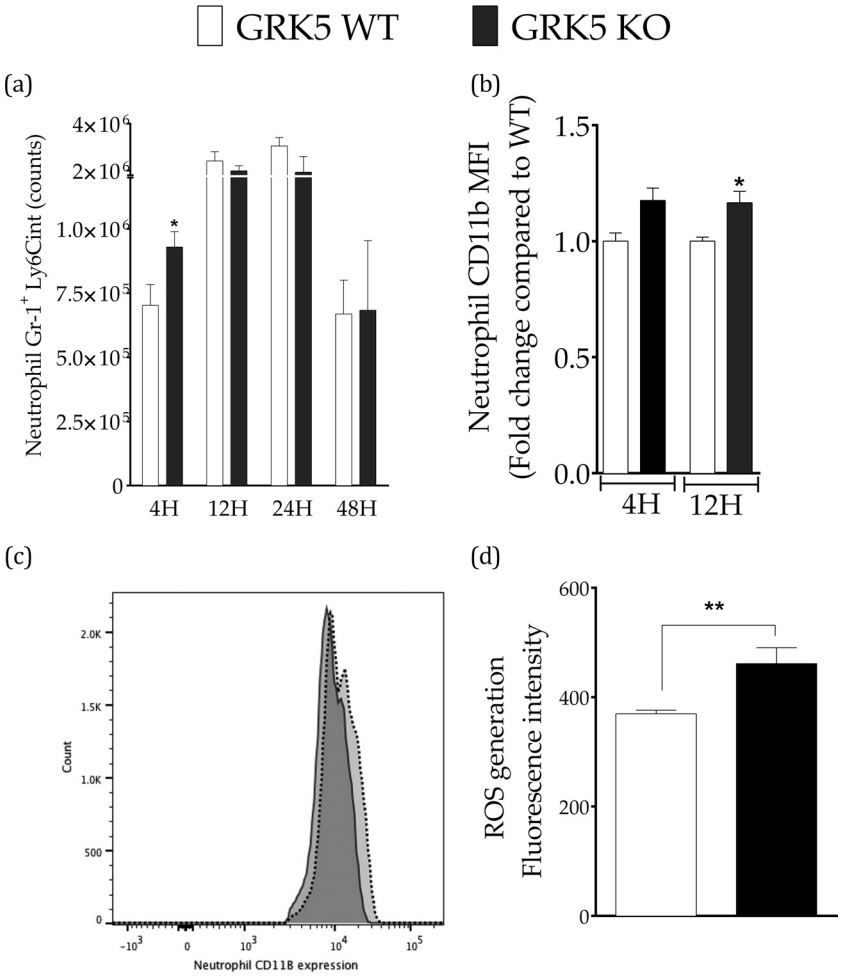

FIG 2 Lung neutrophil recruitment in mice with wild-type (WT) GRK5 and in GRK5 knockout (KO) mice following infection with a sublethal dose of *E. coli*. (a) Lung samples collected at different time points from GRK5 WT and KO mice infected with *E. coli* as described in the legend to Fig. 1 were analyzed for cellular composition by flow cytometry. Only results for neutrophils are shown. The numbers of other immune cells did not differ significantly between mice of different genotypes (data not shown). (Number of animals per group: 8 to 10 at 4 h, 6 to 9 at 12 h, 5 at 24 h, and 5 at 48 h.) An asterisk indicates a significant difference (*, $P < 0.05$) from the corresponding WT group. (b) Lung samples (collected 4 and 12 h postinfection) were also analyzed by flow cytometry for expression (mean fluorescence intensity) of CD11b on the surfaces of neutrophils (number of animals per group: 5 at 4 h and 9 to 13 at 12 h). The difference between the groups was nonsignificant (*P*, 0.095 by a two-tailed test) for the 4-h time point. (c) Representative fluorescence-activated cell sorter (FACS) plot showing CD11b expression on neutrophils at the 12-h time point (solid line, GRK5 WT; dotted line, GRK5 KO). (d) ROS generation was measured by fluorescence from BAL fluid cells (as described in Materials and Methods) 12 h postinfection. Number of animals: 5 per group (**, $P < 0.01$).

RESULTS

GRK5 inhibits bacterial clearance but does not regulate intracellular bacterial killing. To determine the role of GRK5 in bacterial clearance, we infected wild-type (WT) and GRK5 knockout (KO) mice intratracheally with live *E. coli* in the log phase of growth at 1×10^6 CFU/mouse (sublethal dose, determined from pilot experiments). After infection, lung homogenates, bronchoalveolar lavage fluid, and blood samples were prepared at specified time points and were plated onto tryptic soy agar plates, and CFU counts were determined after 24 h. As predicted, *E. coli* at 1×10^6 CFU/mouse induced low-grade infection; bacteria were mostly cleared from the lungs by 24 h postinfection (Fig. 1) and were not detected in the blood at any of the time points tested (data not shown). Mice of both genotypes had comparable bacterial loads early (4 h) after infection, both in the lungs and in BAL fluid (Fig. 1a and b). However, by 12 h postinfection, bacterial counts in the lungs and BAL fluid of GRK5 KO mice were significantly lower than those in WT mice (Fig. 1a and b). These results suggest that GRK5-deficient mice are able to clear bacteria much better than the WT mice.

Bacterial burdens might be regulated by various processes, including phagocytosis, bacterial killing, and/or regulation of phagocyte infiltration. To determine if GRK5 directly regulated phagocytosis or bacterial killing, we performed an *in vitro* intracellular bacterial killing assay using thioglycolate-induced peritoneal neutrophils. As shown in Fig. S1 in the supplemental material, phagocytosis (as seen at the 0-min time point) and intracellular bacterial killing (as seen at the 30- and 60-min time points) were similar for WT and GRK5 KO neutrophils. These data clearly suggest that the reduced bacterial burden observed *in vivo* in KO mice is not likely due to a direct role of GRK5 in phagocytosis or bacterial killing.

GRK5 inhibits early neutrophil recruitment to the lungs. Because our data ruled out a role for GRK5 in bacterial killing, we shifted our focus to understanding the dynamics of immune cell infiltration during bacterial pneumonia *in vivo*. For this purpose, we used flow cytometry to examine the lung tissue for immune cell infiltration. As shown in Fig. 2a, following *E. coli* infection, GRK5-deficient mice had significantly increased numbers of neutrophils in the lungs at 4 h postinfection. Neutrophils were identified as $CD11b^+$ $Gr\text{-}1^{high}$ $Ly6C^{intermediate}$ $F4/80^-$ cells (see Fig. S2 in the supplemental material for the gating strategy) (25, 26). However, at later time points (12 to 48 h), the numbers of neutrophils in the lung were similar for the two genotypes, suggesting that GRK5 influences neutrophil recruitment to the lungs only at early stages during infection. Although statistically significant, the effect on early neutrophil infiltration was small and therefore by itself unlikely to have a large impact on bacterial clearance. Therefore, we examined the activation status of the neutrophils and reasoned that enhanced infiltration combined with a higher activation status of neutrophils could clear bacteria better in the GRK5 knockout mice. To characterize the activation status of these neutrophils, we examined CD11b expression. CD11b expression in neutrophils has been linked to increased reactive oxygen species (ROS) production and increased respiratory burst, which have direct consequences for bacterial killing (27). At both 4 and 12 h postinfection, CD11b expression in GRK5 KO neutrophils was higher than in WT cells (mean fluorescence intensity [MFI] at 4 h, 32,663 arbitrary units [AU] for WT neutrophils and 38,400 AU for KO neutrophils; MFI at 12 h, 36,495 AU for WT neutrophils and 40,677 AU for KO neutrophils [the difference was statistically significant at the 12-h time point]) (Fig. 2b and c). In agreement with the increased CD11b expression, the level of ROS generation was significantly higher in the bronchoalveolar cells from KO mice (Fig. 2d).

Other than the changes in the number of neutrophils described above, we did not observe any major differences between the genotypes in terms of immune cell populations in the lungs (data not shown) except for $CD11b^+$ $Gr1^{high}$ $F4/80^+$ $Ly6C^{intermediate}$ cells (characterized as efferocytosing macrophages) (28). Recently, these cells have also been described as myeloid-derived suppressor cells (MDSCs), which function to restrict ongoing inflammation and favor resolution (28, 29). At 12 h postinfection, the number of cells of this type, which favor resolution, was significantly higher in the lungs of GRK5 KO mice than in those of WT mice (Fig. 3). These data suggest that enhanced neutrophil infiltration and activation, together with an increase in the number of efferocytosing macrophages/myeloid-derived suppressor cells, could favor faster resolution of inflammation, as observed in the GRK5 knockout mice.

GRK5 regulates chemokine ligand but not cell surface chemokine receptor expression. The early increase in neutrophil infiltration in the GRK5 KO mice could be mediated via modulation of chemokine levels and/or through regulation of their respective GPCRs. Therefore, we examined the levels of CXCL1, CXCL2, and MCP1, chemokines known to be regulated during bacterial lung infection. As shown in Fig. 4a, plasma CXCL1 levels were significantly increased in the GRK5 KO mice at 4 h postinfection, but at later time points, mice of the two genotypes exhibited similar levels. Levels of CXCL2 and MCP1 in plasma did not differ significantly between WT and GRK5 KO mice at any of the time points (Fig. 4a). In contrast, levels of these chemokines in

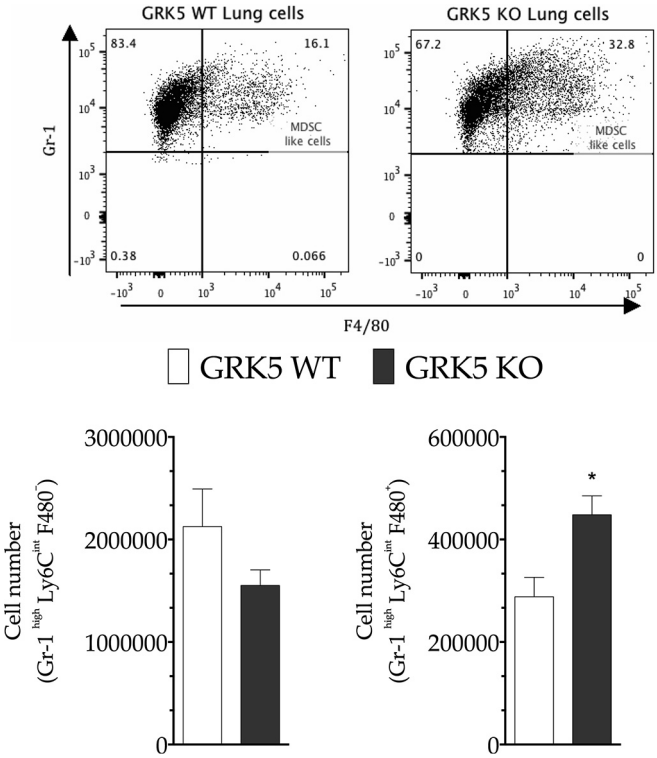

FIG 3 Recruitment of efferocytosing macrophages in mice with wild type (WT) GRK5 and in GRK5 knockout (KO) mice following infection with a sublethal dose of *E. coli*. Lung samples from GRK5 WT and KO mice were collected 12 h after infection with *E. coli* (as described in the legend to Fig. 1), processed, and analyzed by flow cytometry for the presence of $CD11b^+$ $F4/80^+$ $Gr\text{-}1^{high}$ $Ly6C^{intermediate}$ cells. The cells are gated on the $CD11b^+$ and $CD11c^-$ populations. (Top) Results of a representative experiment; (bottom) quantitation of results. (Number of animals: 8 to 10 per group.) An asterisk indicates a significant difference (*, $P < 0.05$) from the corresponding WT group.

BAL fluid were similar for the two genotypes at 4 h postinfection, but at later time points, they were significantly lower in GRK5 KO mice than in WT mice (Fig. 4b).

To assess the role of GRK5 in chemokine receptor expression, we examined the expression of CXCR2 on the surfaces of neutrophils under basal and stimulated conditions in mice of the two genotypes. As shown in Fig. S3 in the supplemental material, CXCR2 expression on the cell surface decreased when the neutrophils were treated with chemokines (likely due to receptor desensitization and internalization). This pattern, however, was similar for the two genotypes under both basal and stimulated conditions. Together, these data suggest that in response to *E. coli* infection, GRK5-deficient mice are able to induce higher plasma CXCL1 levels than WT mice early in the process that may influence neutrophil infiltration.

GRK5 modulates inflammatory status. To assess the inflammatory statuses of the genotypes following bacterial infection, we measured levels of interleukin 6 (IL-6), tumor necrosis factor alpha (TNF-α), IL-12, and IL-10 in the plasma and BAL fluid following *E. coli* infection. As shown in Fig. 5, IL-6 levels were significantly decreased in both the plasma and BAL fluid of KO mice at 12 h postinfection, whereas TNF-α levels were decreased only in plasma at 4 h postinfection. Plasma IL-12 and IL-10 levels were increased/decreased in GRK5 KO mice in a time-dependent man-

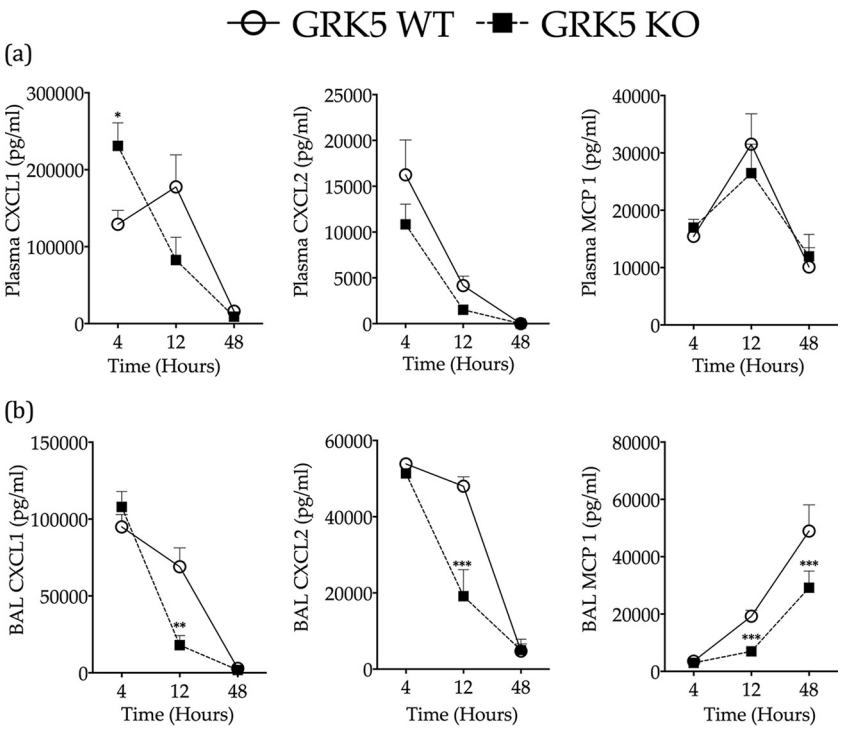

FIG 4 Chemokine levels in the plasma and BAL fluid of mice with wild-type (WT) GRK5 and in GRK5 knockout (KO) mice following infection with a sublethal dose of *E. coli*. GRK5 WT and KO mice were infected with a low dose of *E. coli* as described in the legend to Fig. 1 and were euthanized at various time points as indicated. Plasma (a) and BAL fluid (b) samples were collected and were analyzed for levels of CXCL1, CXCL2, and MCP1. (Number of animals per group: 7 at 4 h, 6 at 12 h, and 4 at 48 h.) Asterisks indicate significant differences (*, $P < 0.05$; **, $P < 0.01$; ***, $P < 0.001$) from the corresponding WT group.

ner (Fig. 5a). However, IL-12 levels were lower, and IL-10 levels were higher, in the BAL fluid of GRK5 KO mice than in that of WT mice (Fig. 5b). Previous studies (10, 19, 20) have shown that GRK5 is a critical regulator of the NF-κB pathway during acute inflammation. To assess the role of GRK5 in the NF-κB pathway in this model, we measured phospho-IκBα levels in the lung tissue. In accord with decreased IL-6 and TNF-α levels in GRK5 KO mice, p-IκBα levels were significantly decreased in KO mouse lung tissue (Fig. 5c).

GRK5 confers a survival advantage following lethal *E. coli* infection. Even though GRK5 KO mice were protected from bacterial burdens and inflammation following sublethal *E. coli* infection, this protection did not result in overt histopathological differences between the genotypes (WT and GRK5 KO) in terms of resolution of inflammation at 48 h postinfection (data not shown). To further understand the role of GRK5 in *E. coli*-induced mortality (a clinically relevant outcome), we administered a lethal dose of *E. coli* to mice of the two genotypes. We hypothesized that since bacterial burdens and inflammation are decreased in GRK5 KO mice, GRK5 deficiency would protect the mice from *E. coli*-induced mortality. The rationale for this hypothesis was also based, in part, on our previous studies with a polymicrobial sepsis model, in which we showed that GRK5 deficiency enhances survival, especially in the presence of antibiotic therapy (19). Therefore, we tested the role of GRK5 with a lethal dose of *E. coli* that we predicted (based on pilot studies) would cause ~50% mortality in WT mice. For this purpose, we used an *E. coli* dose of 5×10^6 CFU/mouse and performed survival studies. Surprisingly, in contrast to our prediction, GRK5 KO mice succumbed to pneumonia much more readily than WT mice (Fig. 6a). At 48 h postinfection, GRK5 KO mice exhibited 90% mortality, compared to 58% mortality for WT mice (Fig. 6a). Also, the median survival for WT mice was 33 h, in contrast to 18 h for GRK5 KO mice. Additionally, histopathological analysis of lung tissue obtained from mice infected with a lethal dose of *E. coli* revealed significant damage in the lungs of KO mice (Fig. 6b; see also Fig. S4 in the supplemental material).

To begin to understand this paradox, we first examined bacterial burdens in this high-dose infection model. In contrast to the results with a sublethal dose of *E. coli*, following lethal *E. coli* infection, GRK5 KO mice showed significantly higher bacterial loads in the lungs and blood than WT mice (Fig. 6c). This suggests that following lethal *E. coli* infection, GRK5 KO mice are unable to clear the bacterial infection. To determine the potential mechanisms, we examined neutrophil infiltration, CD11b expression, and CXCL1 production in mice of the two genotypes following lethal *E. coli* infection. Although neutrophil infiltration (Fig. 7a) and CXCL1 production (only in the plasma [Fig. 7e], not in BAL fluid [see Fig. S5 in the supplemental material]) were enhanced in the GRK5 KO mice comparably to their enhancement with the sublethal dose, CD11b expression was significantly lower in GRK5 KO neutrophils than in WT cells (MFI, 44,937 AU for WT and 38,786 AU for KO neutrophils at 4 h; 57,189 AU for WT and 52,094 AU for KO neutrophils at 12 h; 21,538 AU for WT and 19,208 AU for KO neutrophils at 15 h) (Fig. 7c). Additionally, ROS production from bronchoalveolar cells was significantly lower in GRK5 KO mice than in WT mice (Fig. 7d). Overall, these data suggest that neutrophils from GRK5 KO mice after lethal bacterial infection are likely less activated or exhausted and consequently

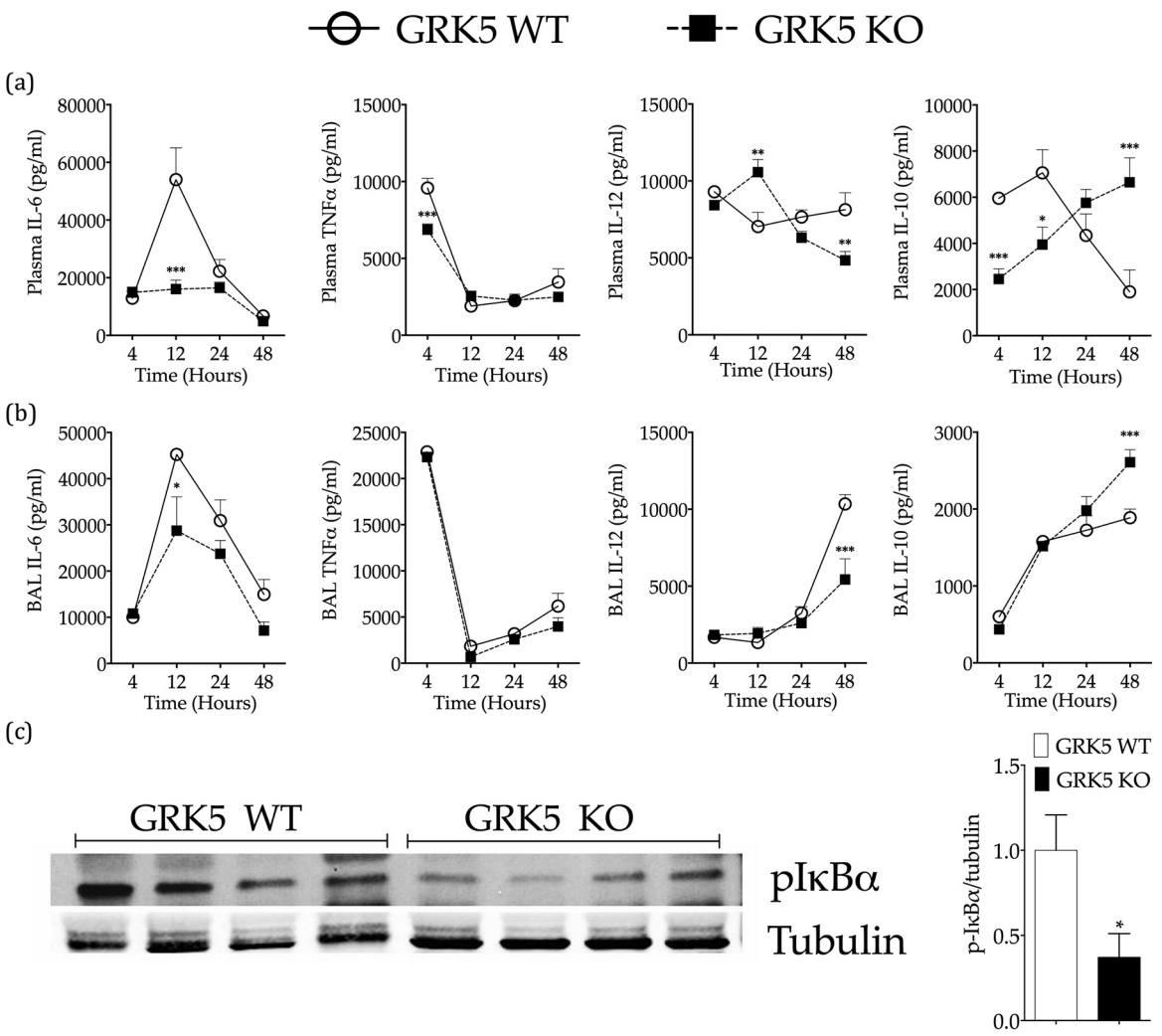

FIG 5 Inflammatory response in mice with wild-type (WT) GRK5 and in GRK5 knockout (KO) mice following infection with a sublethal dose of *E. coli*. GRK5 WT and KO mice were infected with a low dose of *E. coli* as described in the legend to Fig. 1 and were euthanized at various time points after infection. (a and b) Plasma (a) and BAL fluid (b) samples were analyzed for levels of IL-6, TNF-α, IL-12p40, and IL-10. (Number of animals per group: 10 to 15 at 4 h, 9 to 15 at 12 h, 5 at 24 h, and 5 at 48 h.) Asterisks indicate significant differences (*, $P < 0.05$; **, $P < 0.01$; ***, $P < 0.001$) from the corresponding WT group. (c) (Left) Immunoblot showing pIκBα levels in mice with WT GRK5 and GRK5-deficient mice after injection with a low dose of *E. coli*. (Right) Ratio of pIκBα to tubulin. (Number of animals: 4 per group.)

are unable to clear infection efficiently, leading to higher lung damage and mortality.

DISCUSSION

Dysregulated inflammation is a characteristic feature in many inflammatory diseases, including pneumonia and sepsis. Alterations in the initial events of infection, such as detection of the microbe by the host, inflammatory signaling, and chemotaxis of immune cells, can modify the course of disease processes. During lung infection, optimal neutrophil recruitment is critical for clearing bacteria from lungs and for establishing homeostasis (30–32). In previous studies, we demonstrated that a deficiency of GRK5 could protect mice from polymicrobial sepsis-induced mortality, especially in the presence of antibiotics (19). In contrast, in this study, we show that GRK5 plays a paradoxical role in regulating *E. coli*-induced pneumonia, depending on the dose of *E. coli*. While at a sublethal dose of bacteria, GRK5 KO mice are able to clear bacteria better than WT mice, at a lethal dose, KO mice succumb more rapidly than WT mice to bacterial infection. Thus, in direct contrast to the sublethal-dose model, GRK5 KO mice sustain higher bacterial loads than WT mice when administered a lethal dose of *E. coli*. Although neutrophil infiltration *per se* did not differ between the lethal and sublethal doses with respect to GRK5 KO mice, expression of CD11b and ROS production were differentially regulated with the two doses: with the sublethal dose, GRK5 KO mice had higher CD11b expression and ROS production, which were associated with better bacterial clearance, whereas with the lethal dose, GRK5 KO mice had lower CD11b expression and ROS production, and these were associated with poor bacterial clearance. CD11b is an integrin receptor and can significantly influence a number of neutrophil functions, including transmigration, complement receptor pathway activation, and ROS production, all of which are important for reducing bacterial burdens (33). Taken together, our results suggest that neutrophils are less activated in GRK5 KO mice in the lethal-dose model and therefore are unable to clear bacteria effectively. It should be noted, how-

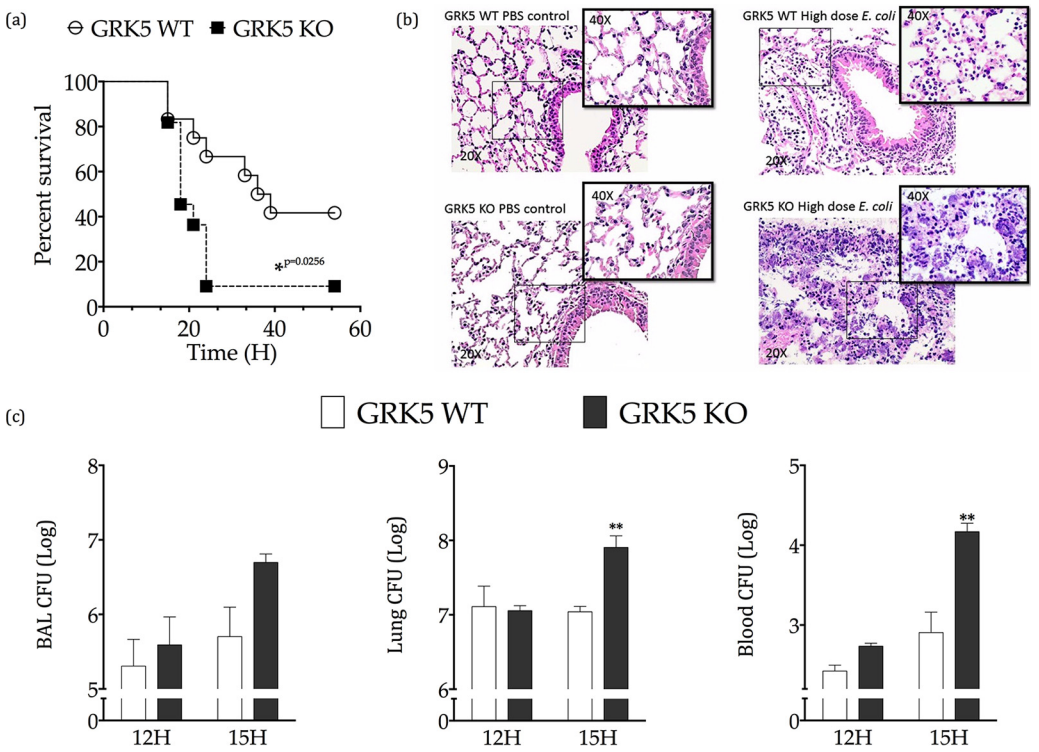

FIG 6 Mortality, lung damage, and bacterial burdens in mice with wild type (WT) GRK5 and in GRK5 knockout (KO) mice following infection with a lethal dose of *E. coli*. (a) GRK5 WT and KO mice were infected intratracheally with *E. coli* at 5×10^6 CFU/mouse. Mice were then monitored for survival as indicated. (Eleven to 12 mice were infected per group.) The asterisk indicates a significant difference (*, $P < 0.05$) from the corresponding WT group. (b) GRK5 WT and KO mice were infected intratracheally with *E. coli* at 5×10^6 CFU/mouse. PBS-treated mice were used as a control. Fifteen hours postinfection, lung tissues were processed for histology. (Left) Lungs from PBS-treated GRK5 WT (top) and KO (bottom) mice. (Right) Lungs from *E. coli*-infected GRK5 WT (top) and KO (bottom) mice. (Insets) Higher magnification (×40) of the slides. Significant histopathological differences were observed between wild-type and knockout mice in the *E. coli*-infected groups. Knockout mice had significantly more areas of necrosis, increased fibrin deposition, and larger foci of bacteria. (c) GRK5 WT and KO mice were injected intratracheally with 5×10^6 CFU of *E. coli*. After the indicated time points, lungs, BAL fluid, and blood were collected and were plated for bacterial growth as described in Materials and Methods. (Number of animals per group: 3 or 4 after 12 h and 5 to 7 after 15 h.) Asterisks indicate significant differences (*, $P < 0.05$; **, $P < 0.01$) from the corresponding infected WT group.

ever, that since the magnitude of the effects is small (though statistically significant), additional mechanisms might be at play.

CXCR2 is a GPCR and is critical for neutrophil recruitment in lung infection (34–36). Based on this, we initially hypothesized that the enhanced neutrophil recruitment in GRK5 KO mice may be driven by higher cell surface expression and activation of CXCR2 in the absence of GRK5. However, our data indicate that GRK5 does not regulate the expression of CXCR2 on the cell surface. Instead, our results suggest that GRK5 is an important regulator of CXCL1, at least in the plasma, early after infection in both the lethal- and sublethal-dose models. The increase in CXCL1 levels in the blood was specific for this compartment, since we did not observe similar increases in the BAL fluid or lungs (see Fig. S5 in the supplemental material). In agreement with this, GRK5 did not regulate CXCL1 production in an *in vitro* lung cell line model (data not shown). Certainly, further extensive studies are necessary to examine if GRK5 regulation of CXCL1 production in the plasma provides enough of a differential gradient for neutrophil recruitment to the lungs. Even though it is well established that the CXCL1/CXCR2 pathway is critical in the recruitment of neutrophils, recent studies demonstrate that CXCL1 monomer-dimer equilibrium can modulate neutrophil recruitment and killing due to distinct activities of these CXCL1 monomers and dimers in the recruitment and activation processes (37). Thus, future studies will examine if GRK5 is able to modulate the monomer-dimer equilibrium and whether this has any functional significance for the outcome of bacterial pneumonia in the sublethal- and lethal-dose models.

Interestingly, in addition to increased bacterial clearance in the sublethal-dose model, GRK5 deficiency also led to an increased proportion of efferocytosing macrophages. These cells are known to clear dying and dead cells (29). Thus, it is likely that the resolution of inflammation could be accelerated in this model. Further, we observed decreased activation of NF-κB in the lungs of GRK5 KO mice, which probably resulted from faster bacterial clearance, and therefore less activation of inflammatory signaling pathways, with the sublethal dose. However, it is also possible that decreased NF-κB activation could be a result of the previously demonstrated role of GRK5 in NF-κB signaling (11, 38). GRK5 has been shown to regulate NF-κB signaling positively (macrophages) (10) or negatively (endothelial cells) (38) and to modulate inflammatory response depending on the cell type involved (39). We have shown that in endotoxemia (20) and polymicrobial sepsis (19), GRK5 mediates cytokine production and GRK5 KO mice exhibit an attenuated inflammatory response.

In conclusion, we demonstrate that GRK5 negatively regulates plasma CXCL1 levels and lung neutrophil recruitment early after infection. While these two events are common to the sublethal and

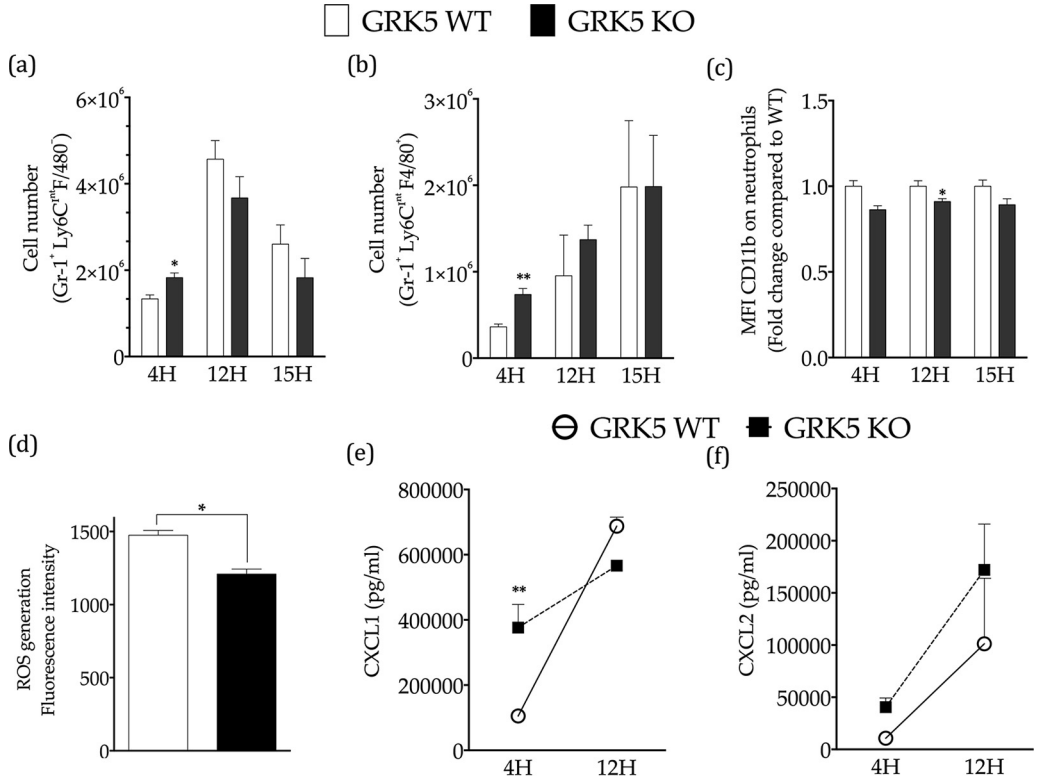

FIG 7 Cellular profiles and chemokine levels in mice with wild-type (WT) GRK5 and in GRK5 knockout (KO) mice following infection with a lethal dose of *E. coli*. GRK5 WT and KO mice were infected intratracheally with a high dose of *E. coli* as described in the legend to Fig. 6, and lung samples were collected at different time points. (a and b) Samples were analyzed for neutrophil (a) and efferocytosing macrophage (b) composition. (Number of animals per group: 3 at 4 h, 3 at 12 h, and 5 at 15 h.) Asterisks indicate significant differences (*, $P < 0.05$; **, $P < 0.01$) from the corresponding infected WT group. (c) Neutrophils were also analyzed for surface expression (mean fluorescence intensity) of CD11b. (Number of animals per group: 3 at 4 h, 4 at 12 h, and 5 at 15 h.) (d) ROS generation was measured by fluorescence from BAL fluid cells (as described in Materials and Methods) 15 h postinfection (number of animals: 5 per group). (e and f) Plasma samples from mice infected with a high dose of *E. coli* were analyzed for levels of CXCL1 and CXCL2. (Number of animals: 3 to 5 per group for each time point indicated.)

lethal doses of *E. coli*, the activation of neutrophils (as assessed by CD11b expression and ROS production) is differentially regulated with these two doses, leading to paradoxical outcomes. Taking these findings together, our study underscores the distinct roles of GRK5 under different infection conditions.

ACKNOWLEDGMENTS

We gratefully acknowledge the support of NIH (grants HL095637, AI099404, and AR056680 to N. Parameswaran).

We thank the university lab animal resources staff for taking excellent care of our animals and the histopathology laboratory for excellent service.

FUNDING INFORMATION

This work, including the efforts of Narayanan Parameswaran, was funded by HHS | NIH | National Institute of Allergy and Infectious Diseases (NIAID) (AI099404). This work, including the efforts of Narayanan Parameswaran, was funded by HHS | NIH | National Heart, Lung, and Blood Institute (NHLBI) (HL095637). This work, including the efforts of Narayanan Parameswaran, was funded by HHS | NIH | National Institute of Arthritis and Musculoskeletal and Skin Diseases (NIAMS) (AR056680).

REFERENCES

1. **Walker CL, Rudan I, Liu L, Nair H, Theodoratou E, Bhutta ZA, O'Brien KL, Campbell H, Black RE.** 2013. Global burden of childhood pneumonia and diarrhoea. Lancet **381:**1405–1416. http://dx.doi.org/10.1016/S0140-6736(13)60222-6.
2. **Kochanek KD, Xu J, Murphy SL, Miniño AM, Kung H-C.** 2011. Deaths: preliminary data for 2009. Natl Vital Stat Rep **59**(4):1–51.
3. **Peleg AY, Hooper DC.** 2010. Hospital-acquired infections due to gram-negative bacteria. N Engl J Med **362:**1804–1813. http://dx.doi.org/10.1056/NEJMra0904124.
4. **Frevert CW, Huang S, Danaee H, Paulauskis JD, Kobzik L.** 1995. Functional characterization of the rat chemokine KC and its importance in neutrophil recruitment in a rat model of pulmonary inflammation. J Immunol **154:**335–344.
5. **Driscoll KE, Hassenbein DG, Howard BW, Isfort RJ, Cody D, Tindal MH, Suchanek M, Carter JM.** 1995. Cloning, expression, and functional characterization of rat MIP-2: a neutrophil chemoattractant and epithelial cell mitogen. J Leukoc Biol **58:**359–364.
6. **Jeyaseelan S, Manzer R, Young SK, Yamamoto M, Akira S, Mason RJ, Worthen GS.** 2005. Induction of CXCL5 during inflammation in the rodent lung involves activation of alveolar epithelium. Am J Respir Cell Mol Biol **32:**531–539. http://dx.doi.org/10.1165/rcmb.2005-0063OC.
7. **Echchannaoui H, Frei K, Letiembre M, Strieter RM, Adachi Y, Landmann R.** 2005. CD14 deficiency leads to increased MIP-2 production, CXCR2 expression, neutrophil transmigration, and early death in pneumococcal infection. J Leukoc Biol **78:**705–715. http://dx.doi.org/10.1189/jlb.0205063.
8. **Packiriswamy N, Parameswaran N.** 2015. G-protein-coupled receptor kinases in inflammation and disease. Genes Immun **16:**367–377. http://dx.doi.org/10.1038/gene.2015.26.
9. **Kunapuli P, Benovic JL.** 1993. Cloning and expression of GRK5: a member of the G protein-coupled receptor kinase family. Proc Natl Acad Sci U S A **90:**5588–5592. http://dx.doi.org/10.1073/pnas.90.12.5588.
10. **Patial S, Luo J, Porter KJ, Benovic JL, Parameswaran N.** 2010. G-protein-coupled-receptor kinases mediate TNFα-induced NFκB signalling

via direct interaction with and phosphorylation of IκBα. Biochem J **425:**169–178. http://dx.doi.org/10.1042/BJ20090908.
11. **Parameswaran N, Pao CS, Leonhard KS, Kang DS, Kratz M, Ley SC, Benovic JL.** 2006. Arrestin-2 and G protein-coupled receptor kinase 5 interact with NFκB1 p105 and negatively regulate lipopolysaccharide-stimulated ERK1/2 activation in macrophages. J Biol Chem **281:**34159–34170. http://dx.doi.org/10.1074/jbc.M605376200.
12. **Valanne S, Myllymaki H, Kallio J, Schmid MR, Kleino A, Murumagi A, Airaksinen L, Kotipelto T, Kaustio M, Ulvila J, Esfahani SS, Engstrom Y, Silvennoinen O, Hultmark D, Parikka M, Ramet M.** 2010. Genome-wide RNA interference in *Drosophila* cells identifies G protein-coupled receptor kinase 2 as a conserved regulator of NF-κB signaling. J Immunol **184:**6188–6198. http://dx.doi.org/10.4049/jimmunol.1000261.
13. **Packiriswamy N, Parvataneni S, Parameswaran N.** 2012. Overlapping and distinct roles of GRK5 in TLR2-, and TLR3-induced inflammatory response in vivo. Cell Immunol **272:**107–111. http://dx.doi.org/10.1016/j.cellimm.2011.10.019.
14. **Funk AJ, Haroutunian V, Meador-Woodruff JH, McCullumsmith RE.** 2014. Increased G protein-coupled receptor kinase (GRK) expression in the anterior cingulate cortex in schizophrenia. Schizophr Res **159:**130–135. http://dx.doi.org/10.1016/j.schres.2014.07.040.
15. **Metaye T, Menet E, Guilhot J, Kraimps JL.** 2002. Expression and activity of G protein-coupled receptor kinases in differentiated thyroid carcinoma. J Clin Endocrinol Metabol **87:**3279–3286. http://dx.doi.org/10.1210/jcem.87.7.8618.
16. **Arraes SM, Freitas MS, da Silva SV, de Paula Neto HA, Alves-Filho JC, Auxiliadora Martins M, Basile-Filho A, Tavares-Murta BM, Barja-Fidalgo C, Cunha FQ.** 2006. Impaired neutrophil chemotaxis in sepsis associates with GRK expression and inhibition of actin assembly and tyrosine phosphorylation. Blood **108:**2906–2913. http://dx.doi.org/10.1182/blood-2006-05-024638.
17. **Agüero J, Almenar L, Monto F, Oliver E, Sanchez-Lazaro I, Vicente D, Martinez-Dolz L, D'Ocon P, Rueda J, Salvador A.** 2012. Myocardial G protein receptor-coupled kinase expression correlates with functional parameters and clinical severity in advanced heart failure. J Card Fail **18:**53–61. http://dx.doi.org/10.1016/j.cardfail.2011.10.008.
18. **Zhang Y, Matkovich SJ, Duan X, Gold JI, Koch WJ, Dorn GW, II.** 2011. Nuclear effects of G-protein receptor kinase 5 on histone deacetylase 5-regulated gene transcription in heart failure. Circ Heart Fail **4:**659–668. http://dx.doi.org/10.1161/CIRCHEARTFAILURE.111.962563.
19. **Packiriswamy N, Lee T, Raghavendra PB, Durairaj H, Wang H, Parameswaran N.** 2013. G-protein-coupled receptor kinase-5 mediates inflammation but does not regulate cellular infiltration or bacterial load in a polymicrobial sepsis model in mice. J Innate Immun **5:**401–413. http://dx.doi.org/10.1159/000347002.
20. **Patial S, Shahi S, Saini Y, Lee T, Packiriswamy N, Appledorn DM, Lapres JJ, Amalfitano A, Parameswaran N.** 2011. G-protein coupled receptor kinase 5 mediates lipopolysaccharide-induced NFκB activation in primary macrophages and modulates inflammation in vivo in mice. J Cell Physiol **226:**1323–1333. http://dx.doi.org/10.1002/jcp.22460.
21. **Nagayama Y, Tanaka K, Hara T, Namba H, Yamashita S, Taniyama K, Niwa M.** 1996. Involvement of G protein-coupled receptor kinase 5 in homologous desensitization of the thyrotropin receptor. J Biol Chem **271:**10143–10148. http://dx.doi.org/10.1074/jbc.271.17.10143.
22. **Mak JC, Chuang TT, Harris CA, Barnes PJ.** 2002. Increased expression of G protein-coupled receptor kinases in cystic fibrosis lung. Eur J Pharmacol **436:**165–172. http://dx.doi.org/10.1016/S0014-2999(01)01625-9.
23. **Rayamajhi M, Redente EF, Condon TV, Gonzalez-Juarrero M, Riches DW, Lenz LL.** 2011. Non-surgical intratracheal instillation of mice with analysis of lungs and lung draining lymph nodes by flow cytometry. J Vis Exp http://dx.doi.org/10.3791/2702.
24. **Sharma D, Packiriswamy N, Malik A, Lucas PC, Parameswaran N.** 2014. Nonhematopoietic β-Arrestin-1 inhibits inflammation in a murine model of polymicrobial sepsis. Am J Pathol **184:**2297–2309. http://dx.doi.org/10.1016/j.ajpath.2014.05.002.
25. **Dunay IR, Fuchs A, Sibley LD.** 2010. Inflammatory monocytes but not neutrophils are necessary to control infection with *Toxoplasma gondii* in mice. Infect Immun **78:**1564–1570. http://dx.doi.org/10.1128/IAI.00472-09.
26. **Rose S, Misharin A, Perlman H.** 2012. A novel Ly6C/Ly6G-based strategy to analyze the mouse splenic myeloid compartment. Cytometry A **81:**343–350. http://dx.doi.org/10.1002/cyto.a.22012.
27. **Chen Y, Mendoza S, Davis-Gorman G, Cohen Z, Gonzales R, Tuttle H, McDonagh PF, Watson RR.** 2003. Neutrophil activation by murine retroviral infection during chronic ethanol consumption. Alcohol Alcohol **38:**109–114. http://dx.doi.org/10.1093/alcalc/agg049.
28. **Poe SL, Arora M, Oriss TB, Yarlagadda M, Isse K, Khare A, Levy DE, Lee JS, Mallampalli RK, Chan YR, Ray A, Ray P.** 2013. STAT1-regulated lung MDSC-like cells produce IL-10 and efferocytose apoptotic neutrophils with relevance in resolution of bacterial pneumonia. Mucosal Immunol **6:**189–199. http://dx.doi.org/10.1038/mi.2012.62.
29. **Ray A, Chakraborty K, Ray P.** 2013. Immunosuppressive MDSCs induced by TLR signaling during infection and role in resolution of inflammation. Front Cell Infect Microbiol **3:**52. http://dx.doi.org/10.3389/fcimb.2013.00052.
30. **Laws TR, Davey MS, Titball RW, Lukaszewski R.** 2010. Neutrophils are important in early control of lung infection by *Yersinia pestis*. Microbes Infect **12:**331–335. http://dx.doi.org/10.1016/j.micinf.2010.01.007.
31. **Sahoo M, Del Barrio L, Miller MA, Re F.** 2014. Neutrophil elastase causes tissue damage that decreases host tolerance to lung infection with *Burkholderia* species. PLoS Pathog **10:**e1004327. http://dx.doi.org/10.1371/journal.ppat.1004327.
32. **Schilter HC, Collison A, Russo RC, Foot JS, Yow TT, Vieira AT, Tavares LD, Mattes J, Teixeira MM, Jarolimek W.** 2015. Effects of an anti-inflammatory VAP-1/SSAO inhibitor, PXS-4728A, on pulmonary neutrophil migration. Respir Res **16:**42. http://dx.doi.org/10.1186/s12931-015-0200-z.
33. **Ramaiah SK, Jaeschke H.** 2007. Role of neutrophils in the pathogenesis of acute inflammatory liver injury. Toxicol Pathol **35:**757–766. http://dx.doi.org/10.1080/01926230701584163.
34. **Nagarkar DR, Wang Q, Shim J, Zhao Y, Tsai WC, Lukacs NW, Sajjan U, Hershenson MB.** 2009. CXCR2 is required for neutrophilic airway inflammation and hyperresponsiveness in a mouse model of human rhinovirus infection. J Immunol **183:**6698–6707. http://dx.doi.org/10.4049/jimmunol.0900298.
35. **Chapman RW, Phillips JE, Hipkin RW, Curran AK, Lundell D, Fine JS.** 2009. CXCR2 antagonists for the treatment of pulmonary disease. Pharmacol Ther **121:**55–68. http://dx.doi.org/10.1016/j.pharmthera.2008.10.005.
36. **Herbold W, Maus R, Hahn I, Ding N, Srivastava M, Christman JW, Mack M, Reutershan J, Briles DE, Paton JC, Winter C, Welte T, Maus UA.** 2010. Importance of CXC chemokine receptor 2 in alveolar neutrophil and exudate macrophage recruitment in response to pneumococcal lung infection. Infect Immun **78:**2620–2630. http://dx.doi.org/10.1128/IAI.01169-09.
37. **Sawant KV, Xu R, Cox R, Hawkins H, Sbrana E, Kolli D, Garofalo RP, Rajarathnam K.** 2015. Chemokine CXCL1-mediated neutrophil trafficking in the lung: role of CXCR2 activation. J Innate Immun **7:**647–658. http://dx.doi.org/10.1159/000430914.
38. **Sorriento D, Ciccarelli M, Santulli G, Campanile A, Altobelli GG, Cimini V, Galasso G, Astone D, Piscione F, Pastore L, Trimarco B, Iaccarino G.** 2008. The G-protein-coupled receptor kinase 5 inhibits NFκB transcriptional activity by inducing nuclear accumulation of IκBα. Proc Natl Acad Sci U S A **105:**17818–17823. http://dx.doi.org/10.1073/pnas.0804446105.
39. **Islam KN, Bae JW, Gao E, Koch WJ.** 2013. Regulation of nuclear factor κB (NF-κB) in the nucleus of cardiomyocytes by G protein-coupled receptor kinase 5 (GRK5). J Biol Chem **288:**35683–35689. http://dx.doi.org/10.1074/jbc.M113.529347.